ACS APPLIED MATERIALS & INTERFACES

Research Article

www.acsami.org

Facile and Scalable Preparation of Solid Silver Nanoparticles (<10 nm) for Flexible Electronics

Yan-Long Tai[†,‡] and Zhen-Guo Yang*[,†]

[†]Department of Materials Science, Fudan University, Shanghai 200433, China

[‡]Physical Sciences and Engineering Division, King Abdullah University of Science and Technology (KAUST), Thuwal 23955-6900, Saudi Arabia

Supporting Information

ABSTRACT: Metal conductive ink for flexible electroncs has exhibited a promising future recently. Here, an innovative strategy was reported to synthesize silver nanocolloid (2.5 ± 0.5 nm) and separate solid silver nanoparticles (<10 nm) effectively. Specifically, silver nitrate ($AgNO_3$) was used as a silver precursor, sodium borohydride ($NaBH_4$) as a reducing agent, fatty acid ($C_nH_{2n+1}COOH$) as a dispersant agent, and ammonia ($NH_3{\cdot}H_2O$) and hydrochloride (HCl) as a pH regulator and complexing agent in aqueous solution. The main mechanism is the solubility changes of fatty acid salts ($C_nH_{2n+1}COO^-NH_4^+$) and fatty acid ($C_nH_{2n+1}COOH$) coated on the synthesized silver nanoparticles (NPs) in aqueous solution. This change determines the suspension and precipitation of silver NPs directly. The results show that when *n* in dispersant is 12 and molar ratio ($C_{12}H_{24}O_2/AgNO_3$) is 1.0, the separation yield of silver NPs is up to 94.8%. After sintering at 125 °C for 20 min, the as-prepared conductive silver nanoink (20 wt %) presents a satisfactory resistivity (as low as 6.6 $\mu\Omega$·cm on the polyester−PET substrate), about 4 times the bulk silver. In addition, the efficacy of the as-prepared conductive ink was verified with the construction of a radio frequency antenna by inkjet printing and conductive character pattern (Fudan−Fudan) by direct wiring, showing excellent electrical performance.

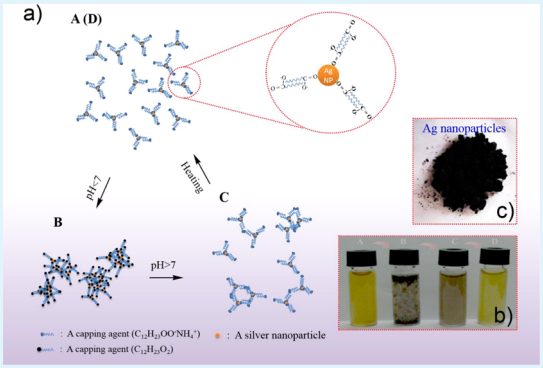

KEYWORDS: *metal conductive ink, flexible electronics, solid silver nanoparticles (<10 nm), radio frequency antenna, conductive character pattern*

1. INTRODUCTION

Recently, many research efforts are being devoted to many kinds of functional inks for flexible electronics, like conductive metal ink,[1,2] dielectric ink,[3,4] magnetic ink,[5,6] ceramic ink,[7,8] semiconductive ink,[9,10] optically active ink,[11,12] thermal sensitive ink,[13] etc. These functional inks can be applied for an electronic skin (E-skin) sensor, organic light-emitting diode (OLED), organic photovoltaic (OPV), flexible battery and supercapacitor, artificial muscles, radio frequency identification (RFID) tags, etc.[14−17] This is mainly because the diverse printing technologies like inkjet printing, screen printing, gravure printing, directing writing, etc. are very promising as additive methods. They will be an important alternative to the production of electronic devices with microscale or millimeter scale, compared with a traditional silicon-based photolithography process. However, these functional inks, especially nanobased inks, are still the main barrier for the application of flexible electronics widely due to their high cost, instability, dilemma of scale production (though some commercial inks, but high price), etc.[18,19] On the basis of these, it is necessary to develop conductive nanometal ink with cost-effective, high quality, easily large-scale production.

Compared with the solid phase method, the liquid phase method is more efficient to prepare metal nanoparticles (NPs) with small size (<10 nm in diameter) and various geometrical morphologies.[20−22] Presently, long-chain fatty acid salts (such as capric acid, lauric acid, myristic acid, oleic acid, etc.) are widely used as dispersants to synthesize metal NPs in aqueous solution. This is because they can be attached onto the surface of metal NPs proficiently by coordinated action between the carbonyl group from fatty acid salts and metal NPs.[18,23,24] Thus, a stable structure of electric double layer can be constructed accordingly, inhibiting the congregation of metal NPs and further forming a steady colloidal solution. However, it is very difficult to separate the nanoparticles from the colloid, and high energy consumption and pollution will be brought based on the present ways, such as centrifugation,[22] nonsolvent precipitation,[25,26] and evaporation.[27,28] Thus, new strategies have to be considered. To the best of our knowledge, there are few studies reporting this work.

Received: April 30, 2015
Accepted: July 2, 2015
Published: July 2, 2015

DOI: 10.1021/acsami.5b03775
ACS Appl. Mater. Interfaces 2015, 7, 17104−17111

Scheme 1. (a) Schematic Illustration for the Separation Process of $C_nH_{2n}O_2$-Coated Silver NPs,[a] (b) the Real-Separation Process, and (c) the As-Separated Solid Silver NPs

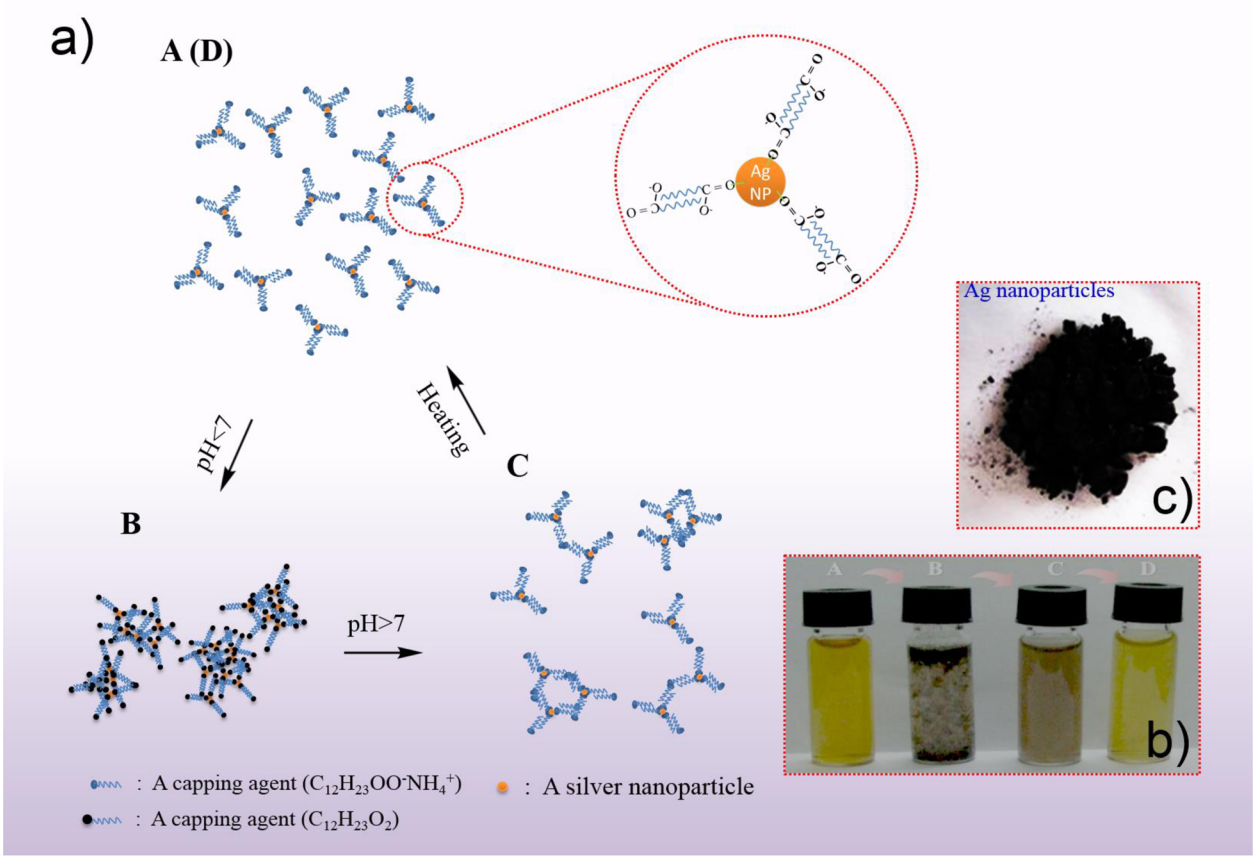

[a]Step-A: stable silver nanocolloid; Step-B: the separation process; Step-C: the redispersion process; Step-D: the protosomatic dispersion.

Herein, a facile and scalable strategy was demonstrated to separate protosomatic metal NPs from its colloid solution effectively. In specific, silver nitrate ($AgNO_3$) was chosen as a silver precursor, sodium borohydride ($NaBH_4$) as reducing agent, fatty acid ($C_nH_{2n+1}COOH$) as dispersant agent, and ammonia ($NH_3{\cdot}H_2O$) and hydrochloride (HCl) as pH regulator and complexing agent in aqueous solution. In this strategy, on one hand, the silver ammonium complex ion $[Ag(NH_3)^{2+}]$ can be obtained from the reaction between $AgNO_3$ and $NH_3{\cdot}H_2O$, which can keep the concentration of the silver ion (Ag^+) stable in solution like a reservoir of Ag^+, as well as regulate the reaction rate well. Meanwhile, fatty acid ammonia ($C_nH_{2n+1}COO^-NH_4^+$) can be obtained from the reaction between $C_nH_{2n+1}COOH$ and $NH_3{\cdot}H_2O$, which is one kind of stronger electrolyte and a good dispersant agent in aqueous solution. It should be noted that $C_nH_{2n+1}COOH$ is insoluble in aqueous solution. On the other hand, if the pH value of the silver nanocolloid was adjusted from alkalinity to acidity by HCl, $C_nH_{2n+1}COO^-NH_4^+$ can change to $C_nH_{2n+1}COOH$. Thus, silver NPs coated by $C_nH_{2n+1}COOH$ precipitate accordingly in aqueous solution. If restoring the pH to alkaline, the precipitated metal nanoparticles can be redispersed. A schematic illustration of the separation process is shown in Scheme 1.

This method is very promising and offers the following advantages: (i) green and environmentally friendly preparation and separation process; (ii) relatively inexpensive starting materials; (iii) excellent electrical properties and good processing adaptability; (iv) easy to accomplish large-scale production. Therefore, this paper will exhibit this promising strategy about the preparation and separation of solid silver NPs. Its efficacy of the as-prepared conductive ink was also verified with the construction of radio frequency antenna by inkjet printing and conductive character pattern (Fudan−Fudan) by direct wiring. Moreover, we envision that this approach can be extended to the synthesis of other metal or nonmetallic nanomaterials and functional application.

2. EXPERIMENTAL SECTION

2.1. Materials. Silver nitrate ($AgNO_3$, ACS, 99.9+ %) was purchased from Alfa Aesar. Polyester (PET) was received from Teonex with the thickness of 125 μm. All the other chemicals were obtained from Shanghai Sinopharm Chemical Reagent Co., Ltd., and were used without further treatment. Deionized water was used in all experimental processes.

2.2. Preparation and Separation of Silver NPs. Preparation of silver nanocolloid: the new prepared $[Ag(NH_3)_2^+]$ solution was mixed with fatty acid, with the pH value of 8−9 adjusted by $NH_3{\cdot}H_2O$, under vigorous stirring at 60 °C for 15 min until the solution became transparent. Then, $NaBH_4$ solution was quickly injected into the above mixture by a syringe. After strongly stirring for 10 min, the color of the solution gradually changed from colorless to light yellow to black, and after aging for 24 h at room temperature, the desired silver colloid was obtained.

Separation of Ag NPs: typically, the pH value of the silver nanocolloid was adjusted from alkalinity (8−9) to acidity (6−7) using HCl (0.1 wt %) drop by drop under vigorous stirring at room temperature, and a flocculent precipitate appeared. Then, it was

DOI: 10.1021/acsami.5b03775
ACS Appl. Mater. Interfaces 2015, 7, 17104−17111

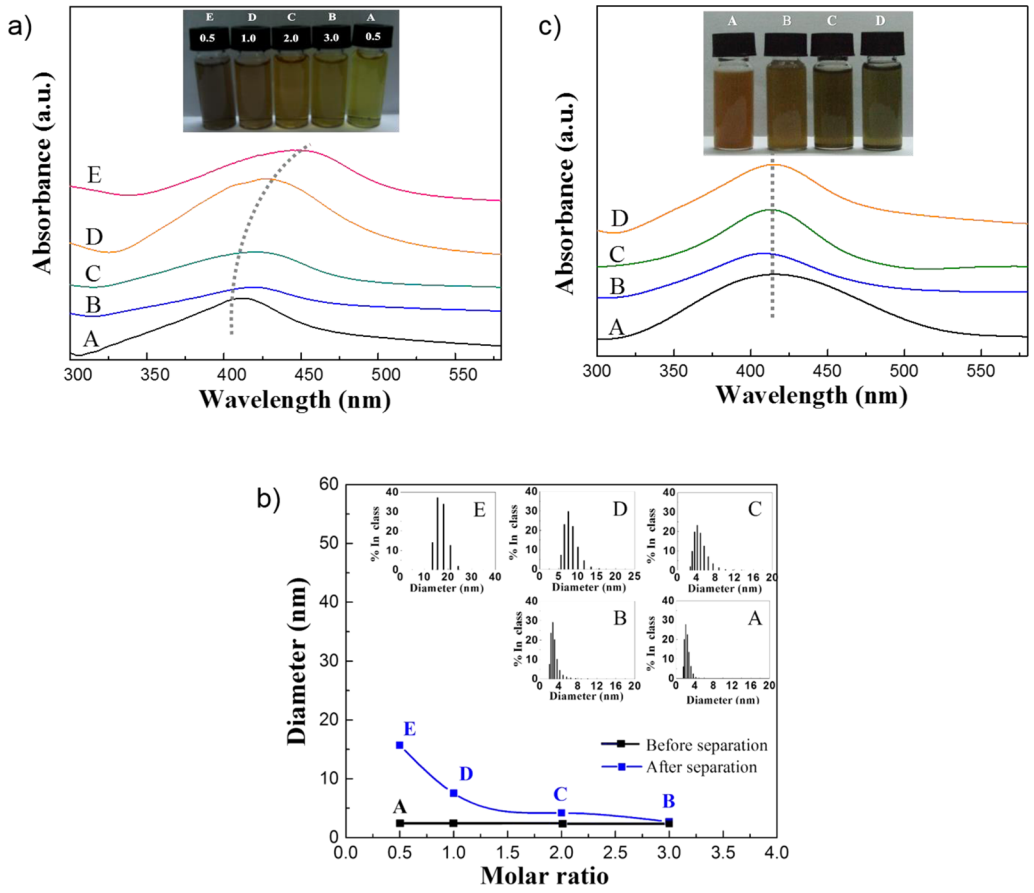

Figure 1. (a) UV−vis absorption spectra of (A) original silver NPs with molar ratio (0.5) and (B, C, D, E) separated silver NPs with molar ratio (3.0, 2.0, 1.0, 0.5, respectively). (b) Size distribution of silver NPs before and after separation with different molar ratios. (c) UV−vis absorption spectra of the separated silver NP with molar ratio (1.0) redispersed in DI water (A), ethanol (B), tetrahydrofuran (C), and dimethylbenzene (D). Inset images are the relevant silver nanocolloids, and the default solvent is DI water. All the molar ratio is $C_nH_{2n+1}COOH/AgNO_3$.

filtered by buchner funnel, along with washing by DI water several times and then vacuum drying for 10 h at room temperature.

2.3. Preparation of Silver Nanoink (20 wt %). The method has been reported before.[18] Briefly, 2 g of the obtained silver NPs was dispersed in 8 mL of an aqueous medium containing ammonia, isopropanol, and ethylene glycol. These solvents were used to adjust to pH = 8, viscosity 10−20 cps, and surface tension 25−40 dyn·cm^{-1} of the silver nanoink, mixing at high speed for 10 min. The prepared conductive ink (20 wt %) can be seen in Section 3.3. The prepared silver ink with lauric acid as dispersant is very stable at least for 10 days without any precipitation.

2.4. Instrumentation. The prepared silver nanocolloid was investigated by an ultraviolet−-vis spectrophotometer (UV−vis 3150, Shimadz, Japan), size analysis (SA, Zeta Nanosizer, Malvern, England), transmission electron microscopy (TEM, JEM-2100F, JEOL, Japan), differential scanning calorimetry (DSC-60, Shimadz, Japan), and X-ray diffraction (XRD, max 2550 PC, Rigaku-D, Japan). The conductive patterns on polyethylene terephthalate (PET) substrate (125 um) were fabricated by piezoelectric drop-on-demand inkjet printer (Fujifilm Dimatix DMP-3000) with the inkjet head of 16 nozzles, 25 um drop distance, and the nozzle voltage of 24−28 V. The printed conductive pattern was measured by a four-point probe (BD-90, Shanghai Power Tool institute, China), scanning electronic microscopy with energy-dispersive X-ray (EDX) analysis (SEM, S-360, Cambridge, England), and a PNA network analyzer (Agilent N5225A, 10 MHz-50 GHz) with a coaxial cable and a subminiature version A (SMA) connector.

3. RESULTS AND DISCUSSION

3.1. Mechanism Consideration. According to the description above, the whole preparation process of solid silver nanoparticles (NPs) in our strategy can be divided into three procedures, including a synthesis process, separation process, and redispersion process, respectively.

For the synthesis process, silver NPs with homogeneous size of 2.5 ± 0.5 nm can be obtained finally through the present method (Section 2.2). This has been confirmed in our previous research.[18] The main chemical reaction during this process can be seen in chemical eqs 1, 2, and 3, in which R_0 is the carbon chain. It is noted that

(1) After the addition of $NH_3{\cdot}H_2O$, not only can it complex Ag^+ to $[Ag(NH_3)^2]^+$ improving its concentration and stability in aqueous solution but also it can react with $C_nH_{2n+1}COOH$ to generate fatty acid ammonia ($C_nH_{2n+1}COO^-NH_4^+$) which is one kind of stronger electrolyte and a good dispersant agent in aqueous solution compared with the poor solubility of $C_nH_{2n+1}COOH$ in water.

(2) Fatty acid or fatty acid salt (normally $10 < n < 18$) can be used as dispersant to synthesize metal nanoparticles due to their strong emulsification ability.[29−31] These are because, on one side, they can form a stable structure of an electric double layer in the relevant solvents due to their amphiphilic groups (carbon chain and carboxyl group). On the other side, they can attach onto the surface of Ag NPs proficiently by chemisorption, and the two oxygen atoms in the carboxylate

DOI: 10.1021/acsami.5b03775
ACS Appl. Mater. Interfaces 2015, 7, 17104−17111

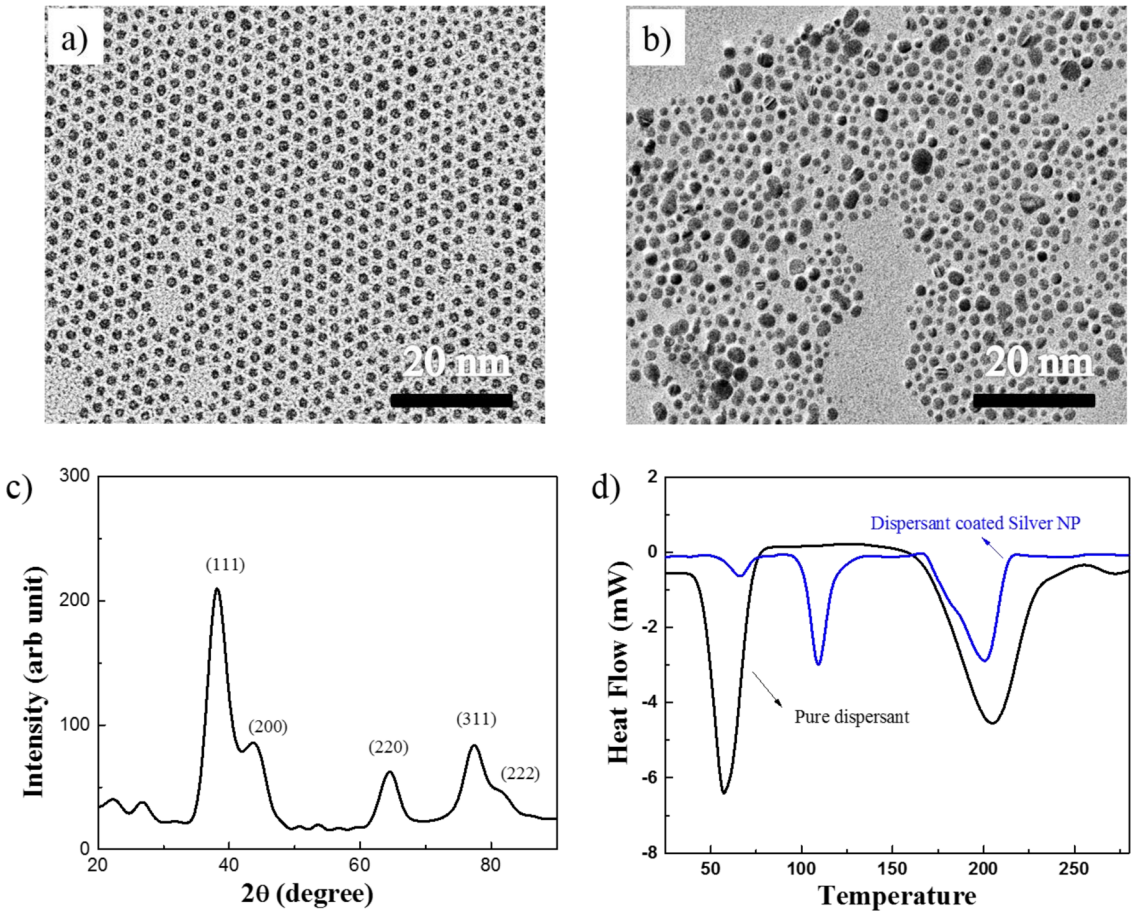

Figure 2. (a) and (b) TEM image of silver NPs before and after separation; (c) XRD of solid silver NPs; and (d) DSC of $C_{12}H_{24}O_2$ and $C_{12}H_{24}O_2$ coated silver NPs (all molar ratio is 1.0).

are coordinated symmetrically to the Ag atoms, leading to the formation of the covalent Ag−O bond.

$$Ag^+(aq) + 2NH_3H_2O \rightarrow [Ag(NH_3)_2]^+(aq) + 2H_2O \quad (1)$$

$$R_0 - COOH + NH_4OH \rightarrow R_0 - COO^-NH_4^+ + H_2O \quad (2)$$

$$Ag^+(aq) \xrightarrow{NaBH_4} Ag \quad (3)$$

For the separation process, how to separate the metal NPs from its colloid is the key point here. The main mechanism is built on the solubility changes of fatty acid salts and fatty acid in aqueous solution. Specifically, $C_nH_{2n+1}COOH$ almost cannot dissolved in water only converting to its relevant salt (like $C_nH_{2n+1}COO^-NH_4^+$) by the adjustment of pH value to alkalinity. On the contrary, when the pH value is back to acidity, $C_nH_{2n+1}COO^-NH_4^+$ will concert to $C_nH_{2n+1}COOH$, precipitating accordingly in water due to its solubility, as shown in Scheme 1b and chemical eq 4. The results indicated that this variation of dispersant dissolution and precipitation does not affect the interaction between the carboxyl group and silver NPs basically. This is ascribed to the stronger interaction between fatty acid and silver NPs through the covalent Ag−O bond.

$$R_0 - COO^-NH_4^+(Ag) + HCl \rightarrow R_0 - COOH(Ag) \downarrow + NH_4Cl \quad (4)$$

For the redispersion process, the obtained silver NP coated $C_nH_{2n+1}COOH$ can be redispersed into aqueous solution if restoring the pH to alkaline, which can be seen in Scheme 1b and chemical eq 5. Noted that high temperature will speed up this redispersing process. Moreover, this kind of silver NP also can be redispersed into other solvents, which can dissolve fatty acid ($C_nH_{2n+1}COOH$). The solubility of dominant saturated fatty acid in various solvents was summarized in Table S1 (Supporting Information). Other fatty acids which can exhibit a similar performance also can be used for the preparation of redispersible solid metal NPs.

$$R_0 - COOH(Ag)(s) + NH_4OH \rightarrow R_0 - COO^-NH_4^+(Ag)(aq) + H_2O \quad (5)$$

Conclusively, based on this synthesis, the separation and redispersion mechanism of solid metal NPs, the following experiments (n = 12 as example) will provide a further verification and optimization systematically.

3.2. Preparation of Solid Silver NPs. To verify the previous mechanism description, silver nanocolloids with different molar ratios of lauric acid ($C_{12}H_{24}O_2$/$AgNO_3$) were prepared.

The UV−vis spectrum was used to discuss the influence of the dispersant dosage on the preparation and separation process. It has been well-known that transition-metal NPs typically exhibit a characteristic surface plasmon absorption band which superimposes onto the exponential decay Mie

DOI: 10.1021/acsami.5b03775
ACS Appl. Mater. Interfaces 2015, 7, 17104−17111

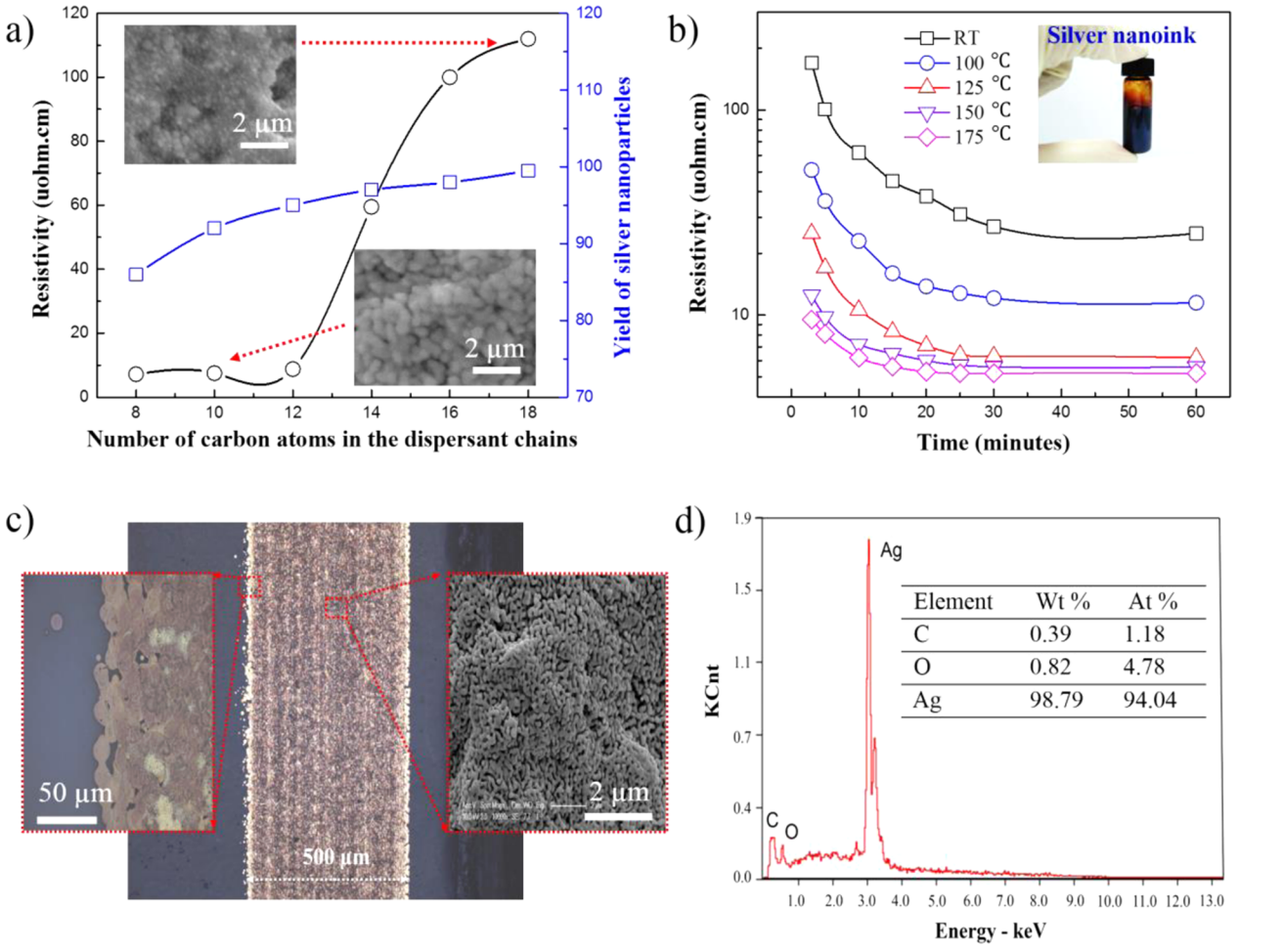

Figure 3. (a) Relationship between resistivity, yield of silver NPs, and the number of carbon atoms in the dispersant (yield = the molar of silver after sintered/that of silver ion, sintering conditions: 125 °C for 20 min). Insets are SEM images of Ag films with different dispersants. (b) Resistivity variations of silver ink (20 wt %) sintered at different temperature and time. Inset is the as-prepared silver nanoink of 20 wt %. (c) Optical and SEM images with different magnifications of silver film. (d) EDX spectrum (taken with SEM). The default dispersant is $C_{12}H_{24}O_2$.

scattering profile. This band intensity is usually proportional to the particle size (volume).[32] As for the silver element, the absorption band at about 310 nm occurs because of Ag^+ ions, whereas the surface plasmon resonance of nanosilver will be at 400 nm or above.

From Figure 1a, it can be seen that all the spectra showed a narrow and intense absorption at 408, 410, 415, 420, and 440 nm corresponding to A, B, C, D, and E, respectively. From the gradual increase of the peak values from A to E, it can be found that the size of the silver NPs is increasing along with the decreasing dosage of $C_{12}H_{24}O_2$. Specially, when the molar ratio is 0.5, the absorption peak of the separated silver nanocolloid shifts to 440 nm. This phenomenon manifests that Ag NPs have the chance to congregate during the conversion process between $C_{12}H_{24}O_2^-NH_4^+$ and $C_{12}H_{24}O_2$. The smaller the dosage of $C_{12}H_{24}O_2$, the larger the chance is.

In addition, size distribution was also used to characterize these processes to present a further confirmation, as shown in Figure 1b. With the decreasing of molar ratio ($C_{12}H_{24}O_2$/$AgNO_3$) from 3 to 0.5, the size of silver NPs after the separation progress increases progressively from 2.69 to 15.70 nm, compared with the original size (2.5 nm) with the molar ratio (0.5). This result is well consistent with that from UV−vis characterization.

The separated silver NPs can be easily redispersed in various solvents which are good for lauric acid ($C_{12}H_{24}O_2$, incl. ethanol, tetrahydrofuran, dimethylbenzene, etc.) or laurate ($C_nH_{2n+1}COO^-NH_4^+$, incl. water, etc.), as seen in Figure 1c. Results present that surface plasmon resonance of nanosilver in different solvents from A to D almost emerges in the scope of 412−417 nm, confirming the above comments. Besides, this phenomenon also should have a relationship with the small size of Ag NPs. Hence, this performance provided a guarantee for the formula optimization of conductive ink to improve its printing suitability.

According to Table S1 (Supporting Information), a different fatty acid ($C_nH_{2n+1}COOH$) displays different solubility, depending on the number of "*n*". Therefore, it is very necessary to select the optimal solvent to optimize the concentration and stability of the final conductive ink in practical applications.

Generally, these results manifest that this strategy is very facile and effective to obtain small size, narrow distribution, and solvent-adaptable Ag NPs.

3.3. Characterization of the Solid Silver NPs. Figure 2a and 2b displays the representative TEM images of silver NPs before and after separation with molar ratio (1.0). It can be seen that the original silver nanoparticle is very uniform with an average size of 2.5 ± 0.5 nm. After the separation and redispersion process, the size of silver NPs becomes a little

DOI: 10.1021/acsami.5b03775
ACS Appl. Mater. Interfaces 2015, 7, 17104−17111

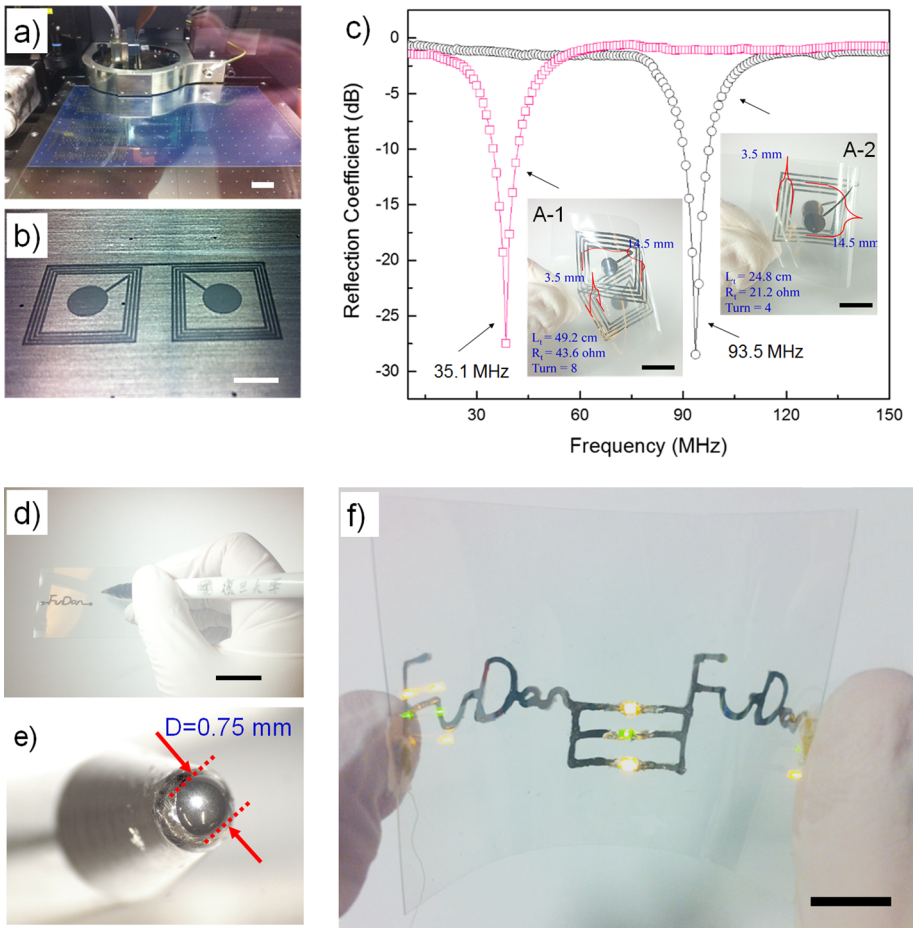

Figure 4. (a) and (b) Digital images for the fabrication of radio frequency antennas (A-1 and A-2) by inkjet printing on PET substrate. (c) Working frequency characterization of two designed radio frequency antennas. (d) and (e) Digital images for fabrication of conductive character pattern (Fudan−Fudan) by direct writing (diameter of pen head is 0.75 mm). (f) Working LED device based on the as-prepared character pattern. Scale bar is 1 cm.

inhomogeneous, where some bigger particles appear, but the average size is still in the range from 4 to 10 nm. It can be concluded that under this molar rate (1.0) the intact bilayer structures of $C_{12}H_{24}O_2$ can inhibit the agglomeration of silver NPs well.

In addition, XRD was used to characterize the crystalline structure of silver NPs as shown in Figure 2c. From the XRD pattern, the prominent peaks at respective 2θ values were exhibited, which presented the (111), (200), (220), (311), and (222) crystal planes of zerovalent fcc silver, respectively, according to Bragg's reflections. Usually, the broadness of the diffraction peaks reflects the size of silver NPs, and the smaller nanoparticles tend to show the broader XRD patterns. Therefore, the line broadening of the X-ray diffraction peaks here was primarily due to the small particle size. These results are consistent with the particle sizes determined by TEM images and size distribution analysis images.

Besides, DSC was also used to investigate the sintering properties of the prepared silver NPs (Figure 2d). It is widely accepted that metal-particle size has a significant impact on its melting point. The smaller the size is, the lower the melting point is. Especially, when the size is down to below 10 nm, the melting point decreases sharply.[33] On the basis of the results, $C_{12}H_{24}O_2$ has two endothermic peaks, at around 58 and 206 °C, which can be indexed as the melting point and boiling point, respectively. Apart from the former peaks, $C_{12}H_{24}O_2$-coated silver NPs have another narrow peak at 105 °C, which can be seen as the melting point of silver NPs. So, it can be inferred that the silver NP prepared by this method is below 10 nm with a narrow distribution.

3.4. Characterization of Conductive Silver Ink. To demonstrate electrical properties of the synthesized silver NPs, silver nanoink with solid content of 20 wt % was prepared, and the resistivity variation and the relationship between resistivity, yield of silver NPs, and the number of carbon atoms in the dispersant were investigated systematically.

From Figure 3a, the dispersant plays an important role in both the synthesis yield of solid silver NPs and the resistivity of silver nanoink. Specifically, when the number of carbon atoms in the dispersant increased from 8 to 18, the yield increased from 86% to 99.5% and the resistivity from 7.2 to 112 $\mu\Omega$·cm after sintering at 125 °C for 20 min. This can be explained that, with the decrease of the carbon number in the dispersant, it is not easier to accomplish the dissolving and precipitating process along with the change of acidity and alkalinity. However, it will be easier to remove the dispersant with shorter carbon chain during the sintering process. This hypothesis can be confirmed from the inset images. The clear and large silver NPs can be seen when the carbon number is 10, compared with the smaller and caking silver NPs when carbon number is 18. In brief, when the number of carbon atoms in the

DOI: 10.1021/acsami.5b03775
ACS Appl. Mater. Interfaces 2015, 7, 17104−17111

dispersant is between 10 and 12, the resistivity and the yield can be balanced well.

Besides, the electrical properties of conductive ink (20 wt %) with carbon number of 12 were further evaluated. From Figure 3b, the resistivity of silver films becomes stable after 20 min. The resistivity was decreased to 10.6 $\mu\Omega$·cm at 100 °C, to 6.6 $\mu\Omega$·cm at 125 °C, and even to 5.1 $\mu\Omega$·cm at 175 °C for 20 min, which is 3.2 times the bulk silver. The microstructure of silver film with different magnifications can be seen from Figure 3c.

The single small particles were melting into larger particles with an average size of 300−600 nm during the sintering process. These large particles connect with each other to fabricate a continuous conductive track, avoiding the scattering of electrons effectively. Moreover, from the chemical composition curve identified by EDX, it also can be obtained that almost all the dispersant has volatilized (Figure 3d). Only three elements (C, O, Ag) can be detected on the surface of the silver thin film: Ag, 98.79 wt %; C, 0.39 wt %; and O, 0.82 wt %.

3.5. Fabrication and Application of the Conductive Pattern. To evaluate the efficacy of the as-prepared silver nanoink (20 wt %) for flexible electronics, two designed radio frequency antennas (A-1 and A-2) were fabricated by an inkjet printer with two layers, as shown in Figure 4a and 4b.[34,35] After sintering at 125 °C for 20 min, the resistance of A-1 (total length L_t = 49.2 cm, turn = 8) and A-2 (total length L_t = 24.8 cm, turn = 4) with line width (500 um) and line spacing (500 um) is 43.6 and 21.2 ohm, respectively. The working frequency of A-1 and A-2 was also measured by a network analyzer (Agilent N5225A) with an SMA connector. Results, summarized in Figure 4c, show that the working frequency peaks are very sharp and clear, 35.1 MHz for A-1 and 93.5 MHz for A-2, indicating the excellent electrical performance.[36] In addition, the efficacy was also demonstrated through the construction of a conductive circuit pattern by direct wiring. A normal gel pen with the diameter of pen head (0.75 mm) was filled with the as-prepared silver nanoink (20 wt %) by syringe. It was used to construct the designed pattern by directing wiring. As shown in Figure 4d and e, a character pattern (Fudan−Fudan) was presented as an example. After three LEDs were integrated into the character pattern and 2.5 V voltage was provided, the LED device worked well.[37,38] Generally, from the above successful exhibitions, it can be concluded that the as-prepared conductive inks can be used for the fabrication of conductive patterns through inkjet printing or direct writing.

CONCLUSIONS

A facile and scalable strategy has been demonstrated to synthesize silver nanocolloids (2.5 ± 0.5 nm) and separate solid silver NPs (<10 nm) successfully, with the main mechanism of the solubility changes of fatty acid salts ($C_nH_{2n+1}COO^-NH_4^+$) and fatty acid ($C_nH_{2n+1}COOH$) in aqueous solution. The results show that when n in dispersant is 12 and molar ratio ($C_{12}H_{24}O_2/AgNO_3$) is 1.0, the separation yield of silver NPs is up to 94.8%. After sintering at 125 °C for 20 min, the as-prepared conductive silver nanoink (20 wt %) presents a satisfactory resistivity (as low as 6.6 $\mu\Omega$·cm on the polyester−PET substrate), about 4 times the bulk silver. Moreover, the construction of radio frequency antenna by inkjet printing and conductive character pattern (Fudan−Fudan) by direct wiring were exhibited to further verify the efficacy of the as-prepared silver nanoink. Generally, this strategy has provided a very promising approach to prepare solid silver NPs (<10 nm) and conductive ink for flexible electronics, which is low cost and environmentally friendly and has easy large-scale production, in addition to its excellent electrical properties and good processing adaptability. In this fashion, this strategy not only can be used for metal NPs but also other metal or nonmetallic nanomaterials and functional applications.

ASSOCIATED CONTENT

Supporting Information

It was found that the solubility of the common fatty acid in main solvents is presented, which can be well used to explain the preparation, separation, and redispersion mechanism of silver NPs coated by fatty acid described in this manuscript. The Supporting Information is available free of charge on the ACS Publications website at DOI: 10.1021/acsami.5b03775.

AUTHOR INFORMATION

Corresponding Author

*E-mail: zgyang@fudan.edu.cn or yanlong.tai@kaust.edu.sa.

Author Contributions

The manuscript was written through contributions of all authors. All authors have given approval to the final version of the manuscript.

Notes

The authors declare no competing financial interest.

ACKNOWLEDGMENTS

We express gratitude to the key discipline fund of Shanghai (B117) for financial support and AKM industrial Ltd for helpful discussions. We would like to thank Prof. Gilles Lubineau for important advice given during the preparation and revision of this manuscript.

REFERENCES

(1) Higgins, S. G.; Boughey, F. L.; Hills, R.; Steinke, J. H. G.; Muir, B. V. O.; Campbell, A. J. Quantitative Analysis and Optimization of Gravure Printed Metal Ink, Dielectric, and Organic Semiconductor Films. *ACS Appl. Mater. Interfaces* **2015**, *7*, 5045−5050.

(2) Almora-Barrios, N.; Novell-Leruth, G.; Whiting, P.; Liz-Marzán, L. M.; López, N. Theoretical Description of the Role of Halides, Silver, and Surfactants on the Structure of Gold Nanorods. *Nano Lett.* **2014**, *14*, 871−875.

(3) Grzelczak, M.; Liz-Marzán, L. M. The Relevance of Light in the Formation of Colloidal Metal Nanoparticles. *Chem. Soc. Rev.* **2014**, *43*, 2089−2097.

(4) Dasgupta, N. P.; Sun, J.; Liu, C.; Brittman, S.; Andrews, S. C.; Lim, J. Semiconductor Nanowires − Synthesis, Characterization, and Applications. *Adv. Mater.* **2014**, *26*, 2137−2184.

(5) Li, N.; Zhao, P.; Astruc, D. Anisotropic Gold Nanoparticles: Synthesis, Properties, Applications, and Toxicity. *Angew. Chem., Int. Ed.* **2014**, *53*, 1756−1789.

(6) Li, X.; Wei, Y.; Lu, L.; Lu, K.; Gao, H. Dislocation Nucleation Governed Softening and Maximum Strength in Nano-Twinned Metals. *Nature* **2010**, *464*, 877−880.

(7) Kumbhar, A. S.; Chumanov, G. Encapsulation of Silver Nanoparticles into Polystyrene Microspheres. *Chem. Mater.* **2009**, *21*, 2835−2839.

(8) Meyers, S. T.; Anderson, J. T.; Hung, C. M.; Thompson, J.; Wager, J. F.; Keszler, D. A. Aqueous Inorganic Inks for Low-Temperature Fabrication of ZnO TFTs. *J. Am. Chem. Soc.* **2008**, *130*, 17603−17609.

(9) Torrisi, F.; Coleman, J. N. Electrifying Inks with 2D Materials. *Nat. Nanotechnol.* **2014**, *9*, 738−739.

DOI: 10.1021/acsami.5b03775
ACS Appl. Mater. Interfaces 2015, 7, 17104−17111

(10) Jin, R.; Cao, Y.; Hao, E.; Gabriella, S.; George, C. S.; Chad, A. M. Controlling Anisotropic Nanoparticle Growth through Plasmon Excitation. *Nature* **2003**, *425*, 487−490.
(11) Park, B. K.; Kim, D.; Jeong, S.; Moon, J.; Kim, J. S. Direct Writing of Copper Conductive Patterns by Ink-Jet Printing. *Thin Solid Films* **2007**, *515*, 7706−7711.
(12) van de Groep, J.; Spinelli, P.; Polman, A. Transparent Conducting Silver Nanowire Networks. *Nano Lett.* **2012**, *12*, 3138−3144.
(13) Li, Y.; Wu, Y.; Ong, B. S. Facile Synthesis of Silver Nanoparticles Useful for Fabrication of High-Conductivity Elements for Printed Electronics. *J. Am. Chem. Soc.* **2005**, *127*, 3266−3267.
(14) Banerjee, S.; Loza, K.; Meyer-Zaika, W.; Prymak, O.; Epple, M. Structural Evolution of Silver Nanoparticles during Wet-Chemical Synthesis. *Chem. Mater.* **2014**, *26*, 951−957.
(15) Anand, U.; Mukherjee, S. Microheterogeneity and Microviscosity of F127 Micelle: The Counter Effects of Urea and Temperature. *Langmuir* **2014**, *30*, 1012−1021.
(16) Su, D.; Wang, G. Single-Crystalline Bilayered V_2O_5 Nanobelts for High-Capacity Sodium-Ion Batteries. *ACS Nano* **2013**, *7*, 11218−11226.
(17) Wang, L.; Chen, Y.; Jiang, J. Controlling the Growth of Porphyrin based Nanostructures for Tuning Third-Order NLO Properties. *Nanoscale* **2014**, *6*, 1871−1878.
(18) Tai, Y. L.; Yang, Z. G. Fabrication of Paper-based Conductive Patterns for Flexible Electronics by Direct-Writing. *J. Mater. Chem.* **2011**, *21*, 5938−5942.
(19) Yang, W.; Liu, C.; Zhang, Z.; Liu, Y.; Nie, S. Copper Inks Formed using Short Carbon Chain Organic Cu-Precursors. *RSC Adv.* **2014**, *4*, 60144−60147.
(20) Pastoriza-Santos, I.; Alvarez-Puebla, R. A.; Liz-Marzán, L. Synthetic Routes and Plasmonic Properties of Noble Metal Nanoplates. *Eur. J. Inorg. Chem.* **2010**, *2010*, 4288−4297.
(21) Hammock, M. L.; Chortos, A.; Tee, B. C. K.; Tok, J. B. H.; Bao, Z. The Evolution of Electronic Skin (E-Skin): a Brief History, Design Considerations, and Recent Progress. *Adv. Mater.* **2013**, *25*, 5997−6005.
(22) Fang, Y.; Lv, Y.; Gong, F.; Wu, Z.; Li, X.; Zhu, H.; Zhou, L.; Yao, C.; Zhang, F.; Zheng, G.; Zhao, D. Interface Tension-Induced Synthesis of Monodispersed Mesoporous Carbon Hemispheres. *J. Am. Chem. Soc.* **2015**, *137*, 2808−2811.
(23) Patil, V.; Sastry, M. Surface Derivatization of Colloidal Silver Particles using Interdigitated Bilayers: a Novel Strategy for Electrostatic Immobilization of Colloidal Particles in Thermally Evaporated Fatty Acid/Fatty Amine Films. *Langmuir* **1998**, *14*, 2707−2711.
(24) Kovalenko, M. V.; Bodnarchuk, M. I.; Lechner, R. T.; Hesser, G.; Schaffler, F.; Heiss, W. Fatty Acid Salts as Stabilizers in Size- and Shape-Controlled Nanocrystal Synthesis: the Case of Inverse Spinel Iron Oxide. *J. Am. Chem. Soc.* **2007**, *129*, 6352−6353.
(25) Liu, X.; Zhang, F.; Huang, R.; Pan, C.; Zhu, J. Capping Modes in PVP-directed Silver Nanocrystal Growth: Multi-Twinned Nanorods versus Single-Crystalline Nano-Hexapods. *Cryst. Growth Des.* **2008**, *8*, 1916−1923.
(26) Yu, Q.; Shan, Z.; Li, J.; Huang, X.; Xiao, L.; Sun, J.; Ma, E. Strong Crystal Size Effect on Deformation Twinning. *Nature* **2010**, *463*, 335−338.
(27) Singh, M.; Haverinen, H. M.; Dhagat, P.; Jabbour, G. E. Inkjet Printing—Process and its Applications. *Adv. Mater.* **2009**, *21*, 673−685.
(28) Shin, D. H.; Woo, S.; Yem, H.; Cha, M.; Cho, S.; Kang, M.; et al. A Self-Reducible and Alcohol-Soluble Copper-based Metal−Organic Decomposition Ink for Printed Electronics. *ACS Appl. Mater. Interfaces* **2014**, *6*, 3312−3319.
(29) Wu, N.; Fu, L.; Su, M.; Aslam, M.; Wong, K.; Dravid, V. P. Interaction of Fatty Acid Monolayers with Cobalt Nanoparticles. *Nano Lett.* **2004**, *4*, 383−386.
(30) Wang, X.; Zhuang, J.; Peng, Q.; Li, Y. A General Strategy for Nanocrystal Synthesis. *Nature* **2005**, *437*, 121−124.
(31) Kumar, A.; Vemula, P. K.; Ajayan, P. M.; John, G. Silver-Nanoparticle-Embedded Antimicrobial Paints based on Vegetable Oil. *Nat. Mater.* **2008**, *7*, 236−241.
(32) Eustis, S.; El-Sayed, M. A. Why Gold Nanoparticles are More Precious than Pretty Gold: Noble Metal Surface Plasmon Resonance and its Enhancement of the Radiative and Nonradiative Properties of Nanocrystals of Different Shapes. *Chem. Soc. Rev.* **2006**, *35*, 209−217.
(33) Lai, S. L.; Guo, J. Y.; Petrova, V.; Ramanath, G.; Allen, L. H. Size-Dependent Melting Properties of Small Tin Particles: Nanocalorimetric Measurements. *Phys. Rev. Lett.* **1996**, *77*, 99−103.
(34) Hart, L. R.; Harries, J. L.; Greenland, B. W.; Colquhoun, H. M.; Hayes, W. Josephine, L. H., Barnaby, W. G.; Howard, M. C.; Wayne, H. Supramolecular Approach to New Inkjet Printing Inks. *ACS Appl. Mater. Interfaces* **2015**, *7*, 8906−8914.
(35) Ellinger, C. R.; Nelson, S. F. Design Freedom in Multilayer Thin-Film Devices. *ACS Appl. Mater. Interfaces* **2015**, *7*, 4675−4684.
(36) Chen, L. Y.; Tee, B. C. K.; Chortos, A. L.; Schwartz, G.; Tse, V.; Lipomi, D. J.; Wong, H. S. P.; McConnell, M. V.; Bao, Z. Continuous Wireless Pressure Monitoring and Mapping with Ultra-Small Passive Sensors for Health Monitoring and Critical Care. *Nat. Commun.* **2014**, *5*, 5028−5036.
(37) Joo, S. J.; Park, S. H.; Moon, C. J.; Kim, H. S. A Highly Reliable Copper Nanowire/Nanoparticle Ink Pattern with High Conductivity on Flexible Substrate Prepared via a Flash Light-Sintering Technique. *ACS Appl. Mater. Interfaces* **2015**, *7*, 5674−5684.
(38) Huang, S.; Zhao, C.; Pan, W.; Cui, Y.; Wu, H. Direct Writing of Half-Meter Long CNT based Fiber for Flexible Electronics. *Nano Lett.* **2015**, *15*, 1609−1614.

DOI: 10.1021/acsami.5b03775
ACS Appl. Mater. Interfaces 2015, 7, 17104−17111